Conformational Differences between Bulged Pyrimidines (C-C) and Purines (A-A, I-I) at the Branch Point of Three-Stranded DNA Junctions†

Mark A. Rosen‡ and Dinshaw J. Patel*,‡,§

Department of Biochemistry and Molecular Biophysics, College of Physicians and Surgeons, Columbia University, New York, New York 10032, and Cellular Biochemistry and Biophysics Program, Memorial Sloan-Kettering Cancer Center, 1275 York Avenue, New York, New York 10021

Received December 9, 1992; Revised Manuscript Received April 8, 1993

ABSTRACT: We have synthesized DNA oligomers that can combine to form three-way junctions containing six base pairs in each stem and two unpaired bases at the branch point. Gel electrophoresis experiments indicate that the oligomers form stable complexes with equimolar stoichiometry. Using two- and three-dimensional proton nuclear magnetic resonance spectroscopy, we have completed nonexchangeable proton chemical shift assignments for three junctions which differ only in the identity of the unpaired bases (C-C, A-A, or I-I) at the branch point. Our results indicate that unpaired pyrimidines at the branch point of junctions behave differently than do unpaired purines. In a junction with two unpaired cytidines, the 5′ base loops out from the molecule to lie along the minor groove of the preceding duplex stem of the junction. The 3′ unpaired cytidine also demonstrates an unusual pattern of NOE connectivities with detected cross peaks to the subsequent base in the 3′ direction. Junctions with unpaired purines at the branch point exhibit different behavior. Our data suggests that in these molecules the unpaired bases participate in stacking interactions among themselves and with the neighboring bases in the molecule. Despite these differences, the NOE patterns from each junction suggest the presence of a preferred, pair-wise stacking between two of the helices within the molecule. The structural differences between bulge–pyrimidine and bulge–purine junctions are discussed in light of the functional significance unpaired bases might have in the structure and dynamics of multistranded DNA junctions and, by extension, to junctions within cellular RNAs.

DNA junctions arise whenever three or more helices come together at a single point. The most frequently encountered DNA junction in biology is the four-stranded, or Holliday, junction (Holliday, 1964). However, simpler junctions comprising just three helices, as well as more complex junctions containing five or six helices, have been described *in vitro* (Ma et al., 1986; Wong et al., 1991).

Holliday junctions are thought to occur within the cell during meiotic recombination (Meselson & Radding, 1975; Orr-Weaver et al., 1981), a process which allows the cell to shuffle genetic material among homologous chromosomes. However, three-stranded DNA junctions are also believed to play a role in certain recombination events (Broker & Doermann, 1975; Mingawa et al., 1983; Jensch & Kemper, 1986). Furthermore, as the simplest junctions, three-stranded junctions can serve as a model for the physical interactions present in Holliday junctions.

When compared with Holliday junctions, three-stranded junctions appear to be more flexible in solution (Ma et al., 1986). There is disagreement in the literature whether the arms in a three-stranded junctions are found in a unstacked, "Y" conformation (Duckett & Lilley, 1990) or in an asymmetric conformation, possibly including base stacking across the branch point (Guo et al., 1990; Lu et al., 1991). However, it is likely that helical stacking in three-stranded junctions, if present, is less stable than that predicted to occur in Holliday junctions.

Chart I

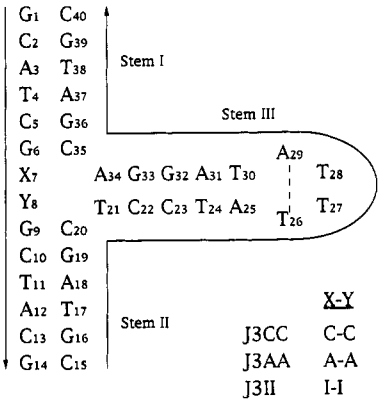

Interestingly, it has recently been shown (Leontis et al., 1991) that three-stranded junctions could be stabilized with the addition to one strand of unpaired, or "bulged", bases at the branch point. The addition of two or more unpaired bases allowed stable three-stranded junctions to form with just five base pairs in each arm. This finding allows one to construct smaller junctions more amenable to detailed structural analysis.

In order to investigate the role of unpaired bases in directing helix–helix interactions within a three-way DNA junction, we have constructed three such junctions, each containing two unpaired bases on one strand at the branch point. The sequence and numbering scheme of the junctions are shown in Chart I. The junctions comprise 17 base pairs (six in two of the arms, five in the other). The three stems are indicated with Roman numerals. One junction, which we call "J3CC", contains two unpaired cytosine bases at the branch point. The second, called "J3AA", contains two adenine bases at this point, whereas "J3II" contains two unpaired inosines. In each

† This research was supported by NIH Grant GM34504 to D.P. M.R. was supported by NIH Medical Scientist Training Program Training Grant 5-T32-GM07376. The NMR spectrometers were purchased from funds donated by the Robert Wood Johnson Trust toward setting up an NMR center in the Basic Medical Sciences at Columbia University.

‡ Columbia University.

§ Memorial Sloan-Kettering Cancer Center.

0006-2960/93/0432-6563$04.00/0

of the molecules, two of the strands have been connected to form a hairpin with a four-base loop.

We have studied these molecules by two- and three-dimensional homonuclear NMR spectroscopy. Our aim was to describe the structural features of the three-way junction with regard to (1) distortions, if any, from the expected B-DNA structure in the double helical regions, (2) the presence or absence of Watson–Crick base pairs adjacent to the branch point, (3) the position and conformation of the unpaired bases, and (4) the overall tertiary structure of the molecules, including the presence of any pair-wise stacking among the three helices.

We present the results of this study in this paper and its accompanying counterpart. In this paper we demonstrate the formation of junction complexes from the component strands and present the sequential ^{1}H-NMR assignments of nonexchangeable protons. In the subsequent paper, we examine the exchangeable proton spectra of J3CC in order to determine the status of the base pairs adjacent to the branch point. We then present a structural model for the J3CC junction that demonstrates the presence of a preferred pair-wise helical stacking arrangement within the molecule.

MATERIALS AND METHODS

DNA Synthesis and Purification. DNA oligomers were synthesized on solid supports (10-μmol scale) using standard phosphoramidite chemistry on an Applied Biosystems 391 automated DNA synthesizer. All reagents were supplied by Applied Biosystems except 5-methylcytidine phosphoramidite, which was supplied by Pharmacia. Oligomers were cleaved from the column and deprotected by treatment with concentrated ammonium hydroxide for 16 h at 55 °C. The trityl-containing oligomers were purified by reverse-phase HPLC, followed by detritylation in 80% acetic acid and repurification through reverse-phase HPLC. Organic cations were removed via gel filtration through Sephadex G-25, followed by passage through a Dowex cation-exchange column to form the Na^+-DNA salt.

DNA Strand Quantification. Oligomer strands were quantified by UV absorbance at 260 nm in 89 mM Tris–borate (pH 8.3) with 200 mM NaCl and 5 mM $MgCl_2$. Extinction coefficients were calculated with consideration of nearest-neighbor effects (Fasman, 1975). Hypochromicity effects were accounted for in the double-stranded hairpin stem region. No attempt was made to correct for the change in extinction coefficient due to the presence of the 5-methylcytidine residue.

Gel Electrophoresis. Gels contained 20% acrylamide (20:1 mono:bis) with 89 mM Tris–borate (pH 8.3), 200 mM NaCl, and either 5 mM $MgCl_2$ or 2 mM EDTA. Samples contained 5–10 μg of either the individual strands or one-to-one mixtures in 10 μL of gel buffer. They were heated to 80 °C for 15 min and allowed to cool slowly to room temperature, following which dye was added, and the samples were loaded onto the gel. The gels were run overnight in a 4 °C cold room, without buffer recirculation, at a constant voltage of 100 V. After electrophoresis was complete, the gels were stained with 5 μg/L ethidium bromide in H_2O for 30 min, followed by destaining for 30 min in distilled H_2O. DNA bands were visualized by transillumination of the gels with 300-nm light and photographed.

Preparation of NMR Samples. Equimolar amounts of the two strands, as determined by gel electrophoresis, were mixed and lyophilized to dryness. The samples were next dissolved in 0.4 mL of 10 mM phosphate buffer (pH 6.2) containing 200 mM NaCl and 0.1 mM EDTA and were heated to 80 °C for 15 min, followed by slow cooling to room temperature. The samples were then repeatedly lyophilized from 99.9% D_2O and were finally dissolved in 0.4 mL of 99.96% D_2O. For some experiments, 5 mM $MgCl_2$ was included through the addition of an aliquot of concentrated $MgCl_2$ in D_2O, followed by reannealing of the strands. Final DNA concentrations were 2-3 mM in each strand.

NMR Spectroscopy. One-dimensional proton NMR spectra were recorded on a Bruker AM-400WB spectrometer. Spectra were acquired with presaturation of the residual HDO peak during the recovery period. The free induction decay, which contained 1024 complex data points, was apodized with a 90° shifted sinebell and zero-filled to 4096 complex points prior to Fourier transformation. All spectra were referenced relative to an internal sodium 4,4-dimethyl-4-silapentane-1-sulfonate (DSS) standard.

Two-dimensional nuclear Overhauser effect spectroscopy (NOESY) experiments were acquired in the phase-sensitive mode (States et al., 1982) on a Bruker AM-500 spectrometer. The two-dimensional data sets were acquired with 1024 complex points in a 10 ppm spectral width in the t_2 dimension. Two different mixing times, 50 and 200 ms, were used in the NOESY experiments. Typically, 256 real and imaginary increments were acquired in the t_1 dimension. The two-dimensional data sets were processed on a VAX/VMS 6310 computer using the software package FTNMR (D. Hare, Hare Research, Inc., Woodinville, WA). The data were subjected to Gaussian multiplication with 12–15 Hz of line narrowing in each dimension. Zero-filling in t_1 led to a matrix with 1024 complex points in each dimension.

A three-dimensional homonuclear NOESY–NOESY experiment was run on a Bruker AMX-600 spectrometer in the phase-sensitive mode using time-proportional phase incrementation (Bodenhausen et al., 1980; Marion & Wuthrich, 1983) in both the t_2 and t_1 dimensions. The pulse scheme used was as reported by Boelens et al. (1989). We used 150 ms for the mixing time in each dimension, with no solvent irradiation during these periods. The matrix comprised 512 × 200 × 110 data points in an 8.0 ppm spectral width. The three-dimensional data set was processed on a Silicon Graphics IRIS using the FELIX software package (D. Hare, Hare Research, Inc., Woodinville, WA). The data was Gaussian multiplied with 12 Hz of line narrowing in each dimension, with zero-filling to a final matrix size of 512 × 256 × 256 complex points.

RESULTS

Formation of Three-Way Junctions. We performed native polyacrylamide gel electrophoresis on mixtures of the different strands to determine whether stable junctions were forming under the experimental conditions. Figure 1 shows the results for a representative gel experiment. Lanes 1 and 2 contain the 14-base oligomers (residues 1–14 in Chart I) with either two cytidines or two adenines in the center. Both oligomers migrate quickly through the gel and stain lightly. The greater retardation of the adenine-containing oligomer may be due to transient formation of homodimers through mismatched base pairing. Lanes 3 and 4 contain bulge-loop duplexes, 12 base pairs in length, formed by one-to-one mixtures of either the cytidine or the adenine 14mer with the "complementary" dodecamer d(CGTAGCCGATGC). The hairpin oligomer alone (residues 15–40 in Chart I) is shown in lane 9. It migrates somewhat more rapidly than either of the two bulged duplexes, suggesting that this molecule does not dimerize under these conditions. We have noted that sequence variants of the

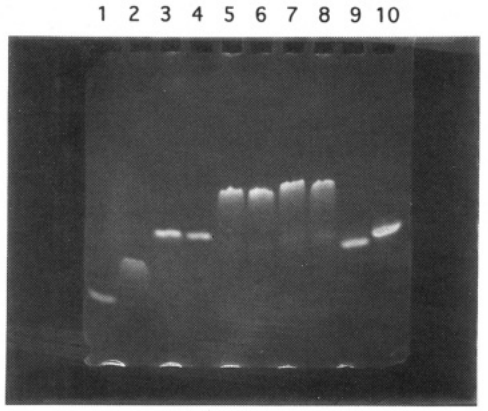

FIGURE 1: Gel electrophoresis experiment showing formation of three-way junctions from component strands. Sample identities are as follows: (1) d(GCATCGCCGCTACG), (2) d(GCATCGAAGCTACG), (3) d(GCATCGCCGCTACG) + d(CGTAGCCGATGC), (4) d(GCATCGAAGCTACG) + d(CGTAGCCGATGC), (5) d(GCATCGCCGCTACG) + d(CGTAGCTCCTA[TTTA]TAGGACGATGC), (6) d(GCATCGAAGCTACG) + d(CGTAGCTCCTA[TTTA]TAGGACGATGC), (7) d(GCATCGCCGCTACG) + d(CGTAGCATCCTA[TTTA]TAGGATCGATGC), (8) d(GCATCGAAGCTACG) + d(CGTAGCATCCTA[TTTA]TAGGATCGATGC), (9) d(CGTAGCTCCTA[TTTA]TAGGACGATGC), (10) d(CGTAGCATCCTA[TTTA]TAGGATCGATGC). Underlined residues represent unpaired bases (CC or AA) within the bulge-duplex or three-way junction complexes. The tetraloop residues from the hairpin strand are enclosed in brackets. Lanes 7, 8, and 10 contain a variant of the hairpin strand with one additional base pair in the stem.

hairpin molecule with an additional GC base pair at the end of the hairpin stem run as a mixture of monomeric and dimeric species on gels (data not shown).

Lanes 5 and 6 represent the three-way junctions, J3CC and J3AA, respectively. These two lanes each show a single, sharp band migrating more slowly than the individual components, confirming the formation of a stable junction in each case. We have compared the mobility of these junctions to that of a larger three-way junction without bulged bases, derived from three separate, unrelated oligomers, each 16 bases in length. This junction runs as a single, sharp band with lower mobility than that of J3CC or J3AA (data not shown), confirming the strand stoichiometry of the J3CC and J3AA junctions.

Ionic Strength Effects on the Stability of the Three-Way Junctions. It has been reported that divalent cations play an important role in the stability and tertiary structure of three- and four-stranded DNA junctions (Cooper & Hagerman, 1989; Duckett et al., 1990; Leontis et al., 1991; Clegg et al., 1992). We have repeated the electrophoresis experiment shown in Figure 1 with 2 mM EDTA instead of 5 mM $MgCl_2$ in the gel buffer. Under these conditions, the junctions appear less stable and are characterized by higher mobility bands or streaks. This confirms the dependence of junction stability on ionic strength.

One-Dimensional Proton Nuclear Magnetic Resonance of the Three-Way Junctions. Figure 2 shows the downfield and methyl regions of the one-dimensional proton NMR spectra in D_2O for the three junctions, J3CC, J3AA, and J3II. DNA strand concentrations are approximately 0.4 mM. Buffer conditions are 200 mM NaCl, 2 mM $MgCl_2$, 10 mM phosphate buffer (pH 6.5), and 0.1 mM EDTA. The resonance lines in the spectra are relatively sharp, implying that stable, one-to-one complexes are forming between the two strands in each case. Minor peaks visible in the spectra may reflect a slightly inequivalent stoichiometry of the two strands in the NMR samples. We noted that as the temperature of the sample was

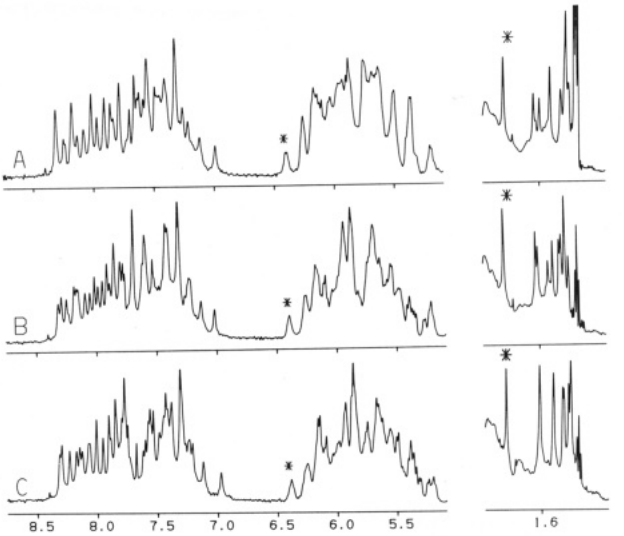

FIGURE 2: One-dimensional proton NMR spectra at 400 MHz of three-way junctions in D_2O buffer (10 mM sodium phosphate, 200 mM NaCl, 2 mM $MgCl_2$, and 0.1 mM EDTA). DNA concentration is approximately 0.4 mM per strand. Base (7.0–8.5 ppm), H1′ (5.2–6.5 ppm), and methyl (1.4–2.2 ppm) regions are shown. (A) Spectrum of J3CC at 25 °C. (B) Spectrum of J3AA at 30 °C. (C) Spectrum of J3II at 30 °C. The asterisks mark the unusual positions of the A29(H1′) and T27(CH_3) resonances in each of the spectra. The triplet at 1.3 ppm represents a residual triethylammonium impurity in the samples.

raised above 35 °C, the minor peaks became more numerous and grew in intensity. By inspecting the NMR spectra of the individual strands (data not shown), we determined that these minor peaks originated from the component oligomers of the junctions. This "melting" effect was even more pronounced at lower NaCl concentrations. Thus, the stability of the junctions seemed to be sensitive to counterion concentration, as was found in gel electrophoresis experiments. Interestingly, the presence of Mg^{2+} cations had no additional stabilizing effect when the NaCl concentration was 200 mM or greater. In fact, the addition of $MgCl_2$ served only to broaden the proton resonance lines in the NMR spectra, indicating transient aggregation of the sample. We therefore elected to proceed with our NMR experiments without $MgCl_2$ in the sample buffer.

The TTTA Loop Retains Its Unique Conformation in the Three-Way Junctions. When joined to a stem of six base pairs, the DNA hairpin loop, 5′-TTTA-3′, posesses a unique conformation, resulting in several unusual proton chemical shifts (Blommers et al., 1991). We find these same chemical shift patterns in the spectra of the three-way junctions. The T27(CH_3) resonance at 1.95 ppm and the A29(H1′) resonance at 6.40 ppm are two such features visible in the one-dimensional spectra of the junctions (asterisks, Figure 2). This result leads us to conclude that the unusual loop structure within the hairpin remains essentially unchanged when part of a larger three-way junction.

NOESY Spectrum of J3CC in D_2O. In order to investigate the structure of the three-way junctions in detail, complete sequential assignments are necessary. These assignments are based on the right-handed nature of the DNA helices, which places proton pairs from neighboring residues within a short distance (<4.5 Å) of each other (Hare et al., 1983; Wuthrich, 1986). Base protons (H8, H6, H5, and CH_3) show NOE connectivities to sugar protons from the same residue, as well as to those from the 5′ preceding residue. As a result, one can start at the 5′ end of a normal B-DNA strand and, by following the pattern of NOE connectivities, "walk" down the helix

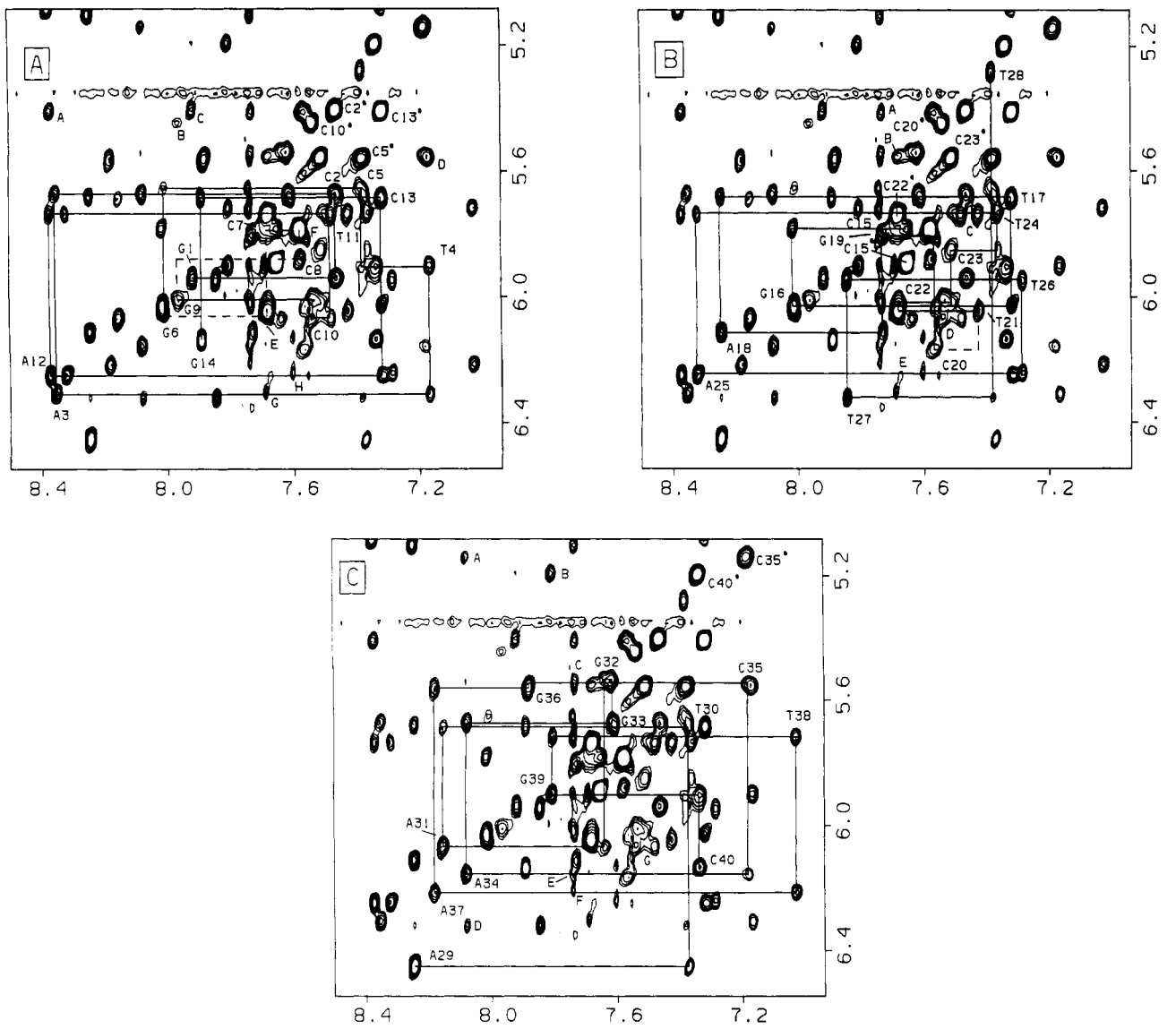

FIGURE 3: Expanded contour plot of the NOESY experiment (200-ms mixing time) on J3CC in D_2O buffer at 25 °C. DNA strand concentration is approximately 2 mM. The base to H1′ region of the spectrum is shown. Sequential assignments are indicated separately in three panels for clarity. Intraresidue base (H8 or H6) to H1′ NOE cross peaks are labeled by residue. Asterisks refer to the cytosine H6–H5 cross peaks. Dotted lines represent sequential connectivities that are absent or are unconfirmed due to the presence of overlapping cross peaks. Assignments for the remaining labeled cross peaks are as follows. Panel A (residues 1–14): (A) A12(H8)–C13(H5), (B) G9(H8)–C10(H5), (C) G1-(H8)–C2(H5), (D) T4(H6)–C5(H5), (E) C7(H6)–C7(H5), (F) C8(H6)–C8(H5), (G) A3(H2)–A3(H1′), (H) A12(H2)–A12(H1′). Panel B (residues 15–28): (A) G19(H8)–C20(H5), (B) C22(H6)–C23(H5), (C) T21(H6)–C22(H5), (D) A18(H2)–A18(H1′), (E) A25(H2)–A25(H1′). Panel C (residues 29–40): (A) A34(H8)–C35(H5), (B) G39(H8)–C40(H5), (C) A34(H2)–C35(H1′), (D) A29(H2)–T27(H1′), (E) A34(H2)–A34(H1′), (F) A37(H2)–A37(H1′).

until one arrives at the 3′ terminal residue [for reviews, see Patel et al. (1987) and van de Ven and Hilbers (1988)].

Figure 3 shows the base to H1′ region of a NOESY experiment (200-ms mixing time) on J3CC in D_2O buffer at 25 °C. The sequential assignments are shown separately in panels A–C for the three "strands" of the molecule. (Residues 15–28 and 29–40 are considered separately due to the break in NOE connectivities between T28 and A29.)

For the majority of the residues falling within the duplex regions of the molecule, the connectivity patterns in the NOESY spectra are unremarkable. All NOEs expected for right-handed DNA helices are visible. The NOE cross-peak intensities clearly indicate that the helices adopt a B-DNA conformation within the junction. This result is in agreement with circular dichroism (Seeman et al., 1984; Marky et al., 1987) and proton NMR (Chen et al., 1991) studies of four-stranded DNA junctions, in which the helices were judged to resemble B-DNA. Overall, the NOE buildup rates appear to be quite rapid. Many NOE connectivities between relatively distant proton pairs, such as intraresidue H8/H6–H1′ or interresidue H2′–H6/H8, could be seen clearly in a 50-ms-mixing-time NOESY experiment. This is most likely attributable to the large size of the molecule, since slow tumbling rates in solution lead to rapid NOE buildups and more efficient spin diffusion.

NOE Interactions at the Branch Point of J3CC. The most interesting observations regarding the NOE connectivities within the first strand of J3CC (residues 1–14, Figure 3A) center on the two unpaired bases, C7 and C8. The H5 proton chemical shifts from both of these residues (6.04 ppm for C7, 5.78 ppm for C8) are located further downfield than are those from any of the other cytosine bases in the molecule, save for C15, a 5′-terminal residue. Sequential NOE connectivities between G6 and C7 are obscured in all regions of the spectrum due to cross-peak overlap. However, the downfield chemical shifts of both the H6 and H5 protons of C7 suggest that there

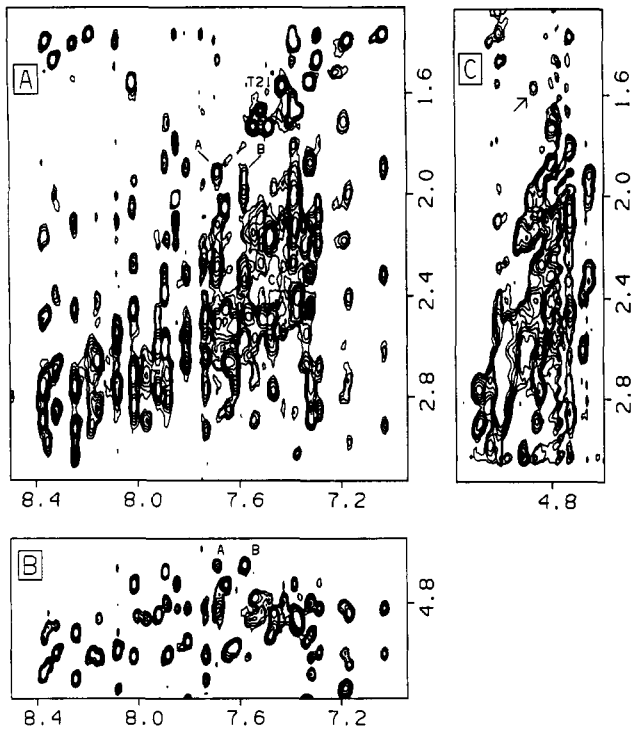

FIGURE 4: Expanded contour plots of NOESY experiments on J3CC in D_2O buffer at 25 °C. (A) Base to H2′/2″ and methyl region (200-ms mixting time). The T21(H6)–T21(CH_3) cross peak is indicated with an asterisk. Cross peak A represents the C7(H2′)–C7(H6) NOE. Cross peak B represents the C7(H2′)–C8(H6) NOE. The C20(H2′/2″)–T21(H6) cross peaks are labeled C in the figure. (B) Base to H3′ region of the spectrum (200–ms mixing time). Two cross peaks (A and B) are labeled at ω1 = 4.65 ppm. In the ω2 dimension, peak A corresponds to C7(H6) (7.68 ppm), while peak B corresponds to C8(H6) (7.57 ppm). (C) H3′ to H2′/2″ and methyl region of the NEOSY spectrum (50-ms mixing time). The C20-(H3′)–T21(CH_3) cross peak is indicated with an arrow.

has been a disruption of base stacking between this residue and G6. For the C7-C8 base step, a single sequential connectivity is resolved in the H2′/2″ region. This cross peak is indicated in Figure 4A. Between residues C8 and G9, all NOEs expected for a normal base step in B-DNA are weak or absent.

The intraresidue H8 to H1′ NOE cross peaks of both G6 and G9 are quite weak. The diminished cross-peak volumes are apparently due to broadening of these resonances in the molecule. This observation suggests the possible existence of a conformational equilibrium between two or more states within this region of the molecule. This dynamic aspect of the junction might be attributable to the increased mobility of one or both of the two unpaired cytidine residues.

The sequential assignments for the second "strand" (residues 15–28, Figure 3B) are unremarkable, except for the C20-T21 base step where the H1′–H6 NOE is quite weak (not visible at the contour level of the figure). The H2′/2″–H6 connectivities for this step are also quite weak and are only seen at the longer mixing time (Figure 4A). Base–base connectivities that would normally be expected for a C-T step (H6–H6, H6–Me, H5–Me) are either weak or absent as well. Interestingly, the C20(H3′)–T21(Me) connectivity is seen quite strongly, even in the NOESY experiment with a short (50 ms) mixing time (Figure 4C). These results imply that the stacking interaction between these two bases has been disrupted and that a unique backbone conformation exists at this step.

The junctional base step of the third strand, A34-C35, shows a number of strong sequential NOE connectivities in the NOESY spectrum. Two of these, A34(H1′)–C35(H6) and A34(H8)–C35(H5), are visible in Figure 3C. NOE connectivities between A34 and C35 are present in every region of the spectrum. In all, we see a total of 16 interresidue NOEs for this base step, making it the most strongly interacting pair of residues at the branch point site of J3CC.

Table I: Nonexchangeable Proton Chemical Shift Assignments for the J3CC Junction in D_2O Buffer at 25 °C

	chemical shifts (ppm)						
base	H6/H8	H5/CH_3	H2	H1′	H2″	H2′	H3′
G1	7.91			5.93	2.77	2.61	4.84
C2	7.46	5.40		5.67	2.48	2.16	4.89
A3	8.35		7.69	6.30	2.98	2.73	5.04
T4	7.16	1.40		5.89	2.41	2.01	4.84
C5	7.38	5.56		5.64	2.27	1.95	4.85
G6	8.01			6.05	2.64	2.53	4.72
C7	7.68	6.04		5.79	2.28	1.92	4.65
C8	7.57	5.78		5.87	2.33	1.99	4.65
G9	7.96			6.00	2.89	2.71	4.86
C10	7.53	5.44		6.06	2.56	2.15	4.78
T11	7.48	1.73		5.73	2.49	2.18	4.93
A12	8.37		7.60	6.24	2.89	2.76	5.08
C13	7.31	5.40		5.68	2.31	1.87	4.80
G14	7.88			6.13	2.39	2.60	4.67
C15	7.65	5.88		5.78	2.45	2.05	4.72
G16	8.01			6.02	2.83	2.71	5.01
T17	7.31	1.55		5.68	2.45	2.12	4.91
A18	8.24		7.55	6.11	2.92	2.76	5.10
G19	7.73			5.80	2.64	2.48	5.01
C20	7.56	5.41		6.16	2.47	2.28	4.86
T21	7.42	1.57		6.04	2.54	2.12	4.79
C22	7.67	5.73		6.01	2.50	2.27	4.83
C23	7.51	5.55		5.84	2.48	2.10	4.7
T24	7.36	1.67		5.73	2.39	2.02	4.9
A25	8.32		7.67	6.24	2.86	2.68	4.99
T26	7.28	1.47		5.94	2.19	2.09	4.82
T27	7.84	2.02		6.31	2.11	1.79	4.72
T28	7.38	1.38		5.27	2.00	1.65	4.45
A29	8.24		8.07	6.45	3.28	3.02	4.91
T30	7.37	1.41		5.68	2.41	2.12	4.86
A31	8.15		7.50	6.06	2.84	2.65	5.0
G32	7.63			5.53	2.66	2.52	4.97
G33	7.61			5.67	2.74	2.52	4.97
A34	8.07		7.7	6.15	2.79	2.60	4.99
C35	7.18	5.14		5.54	2.18	1.71	4.81
G36	7.88			5.56	2.81	2.72	5.00
A37	8.18		7.74	6.21	2.91	2.61	5.00
T38	7.02	1.37		5.71	2.31	1.8	4.82
G39	7.80			5.89	2.66	2.54	4.95
C40	7.33	5.19		6.13	2.20	2.20	4.47

We also note the unusual upfield position of the C35(H5) resonance at 5.14 ppm. In DNA, chemical shift changes are exquisitely sensitive to base-stacking interactions, as the strong ring current effect from purines can alter the electronic shielding of nearby nuclei. It is quite possible that the upfield chemical shift of this H5 proton is due to its stacking under the base moiety of A34. These results suggest that stacking interactions are intact within the A34-C35 base step.

The chemical shifts of all nonexchangeable protons assigned for the J3CC junction in D_2O buffer at 25 °C are listed in Table I.

Three-Dimensional Homonuclear Spectroscopy of J3CC. Since so many of the NOE connectivities in the NOESY spectrum of J3CC were at least partially obscured by overlapping cross peaks, we ran a three-dimensional, homonuclear NOESY–NOESY experiment on this junction. This allowed us to confirm the sequential assignments completed from the two-dimensional NOESY spectra As an example, in the base to H3′ region of the NOESY experiment (Figure 4B), two cross peaks at ω1 = 4.65 ppm (A and B) are indicated. In the ω2 dimension, peak A aligns with the H6 proton of C7, whereas peak B aligns with that of C8. This result poses

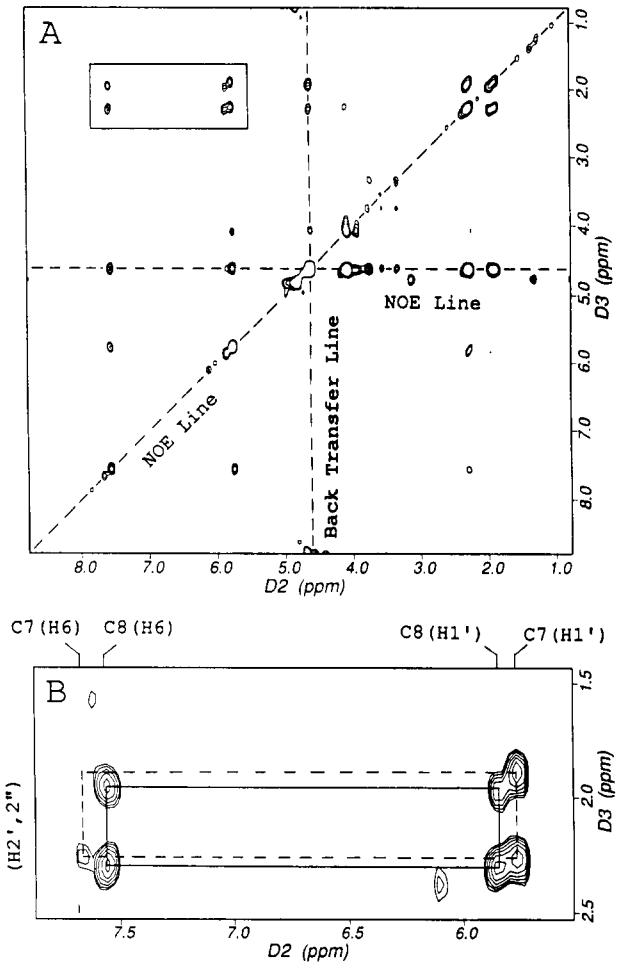

FIGURE 5: (A) Contour plot of a two-dimensional slice ($\omega 1$ = 4.65 ppm) from the three-dimensional homonuclear NOESY–NOESY experiment on J3CC in D_2O buffer at 25 °C. This slice corresponds to the $\omega 1$ position of cross peaks A and B in Figure 4B. (B) Expansion of the boxed region of the contour plot in panel A. The base to H2′/2″ and H1′ to H2′/2″ regions are shown. The assignments for the cross peaks are indicated. The presence of two sets of H1′–H2′/2″ cross peaks confirms that both C7(H3′) and C8(H3′) resonate at 4.65 ppm. The absence of strong cross peaks for C7(H6)–C7(H2′/2″) indicates that this nucleotide adopts an unusual conformation in the junction.

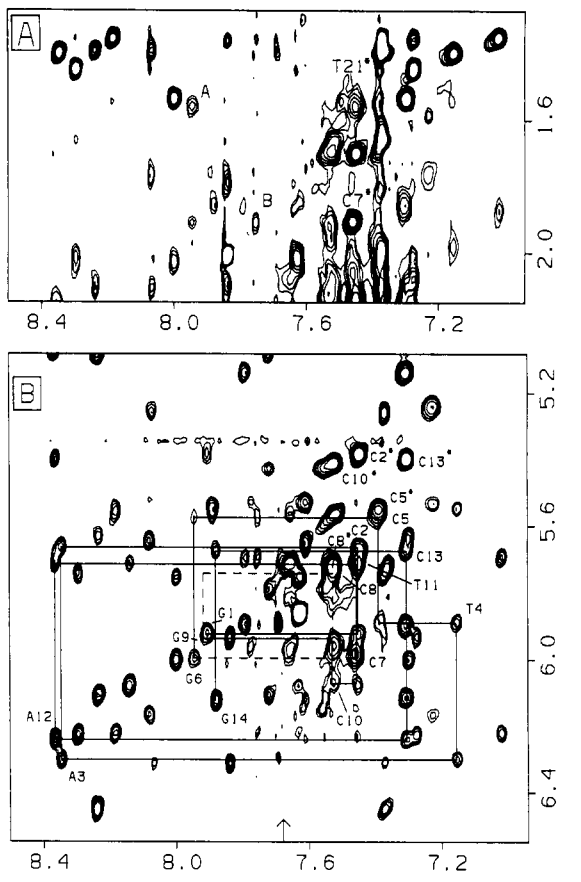

FIGURE 6: Expanded contour plots of a NOESY experiment (200-ms mixing time) on the methylated J3CC junction in D_2O buffer at 25 °C. (A) The base to methyl region is shown. The H6-CH_3 NOEs for residues C7 and T21 are labeled with asterisks. Two interresidue NOEs obscured in the NOESY spectrum of the original molecule are also indicated. Cross peak A represents the G6(H8)–T21(CH_3) NOE, whereas peak B represents the A37(H2)–C7(CH_3) NOE. (B) Base to H1′ region of the same experiment. The sequential connectivities for residues 1–14 are labeled in the figure. Cytidine H5–H6 cross peaks are labeled with an asterisk. The arrow on the lower horizontal axis indicates the approximate position of C7(H6) in the original J3CC junction.

a question as to whether these cross peaks represent intra- or interresidue NOEs, or a combination of the two. In Figure 5A, the $\omega 1$ = 4.65 ppm plane of the three-dimensional NOESY–NOESY experiment on J3CC is shown. An expanded region of this plane demonstrating the base–H2′/2″ and the H1′–H2′/2″ cross peaks is shown in Figure 5B. Two sets of H1′–H2′/2″ NOE cross peaks, belonging to C7 and C8, are labeled in the figure. We therefore conclude that both C7(H3′) and C8(H3′) resonate at 4.65 ppm and that cross peaks A and B in Figure 4B each represent an intraresidue NOE, though interresidual contributions to the NOE intensity may be present as well.

Also shown in Figure 5B are the H6–H2′/2″ cross peaks for C7 and C8. It is clear from the figure that these NOEs are qualitatively different; the cross peaks from C7 are weak or absent. For a nucleotide in the normal B-form conformation (C2′-endo sugar pucker), the H3′–H2′–H6 spin diffusion pathway should be quite efficient. This is not the case for C7, and so we conclude that this residue adopts an unusual geometry, in agreement with our previous findings from the NOESY spectra.

Two-Dimensional NMR Spectroscopy of J3CC with a 5-Methylcytidine at Position 7. We prepared an analogue of the J3CC junction in which the first unpaired base, C7, was replaced by a 5-methylcytidine residue. Our purpose in this endeavor was to confirm the absolute assignments for C7 and C8 in the original junction. These assignments were based solely on the observation of a single sequential NOE in the base to H2′/2″ region of the NOESY spectrum (Figure 4A). Since these bases are most likely found in a nonstandard geometric configuration, the accuracy of these assignments could be called into question.

We ran a NOESY experiment (200-ms mixing time) in D_2O buffer at 25 °C on the new junction with a 5-methylcytidine residue. Contour plots of the base to H1′ and base to methyl regions of this spectrum are shown in Figure 6. From the results, it is immediately evident that our initial assignments are correct. In J3CC, the cytosine base with the most downfield shifted base protons (H6 = 7.68 ppm, H5 = 6.04 ppm) belonged to C7 (peak E, Figure 3A). In the NOESY spectrum of the new junction molecule (Figure 6B), this cross peak has disappeared. The H6 proton of 5Me–C7 is now located at 7.47 ppm. This upfield shift of 0.21 ppm is similar to that seen for H6 protons from model pyrimidine compounds when they are methylated at the C5 position (Fasman, 1975).

In the base to methyl region of the NOESY experiment on the methylated J3CC analogue (Figure 6A), the strong C7-

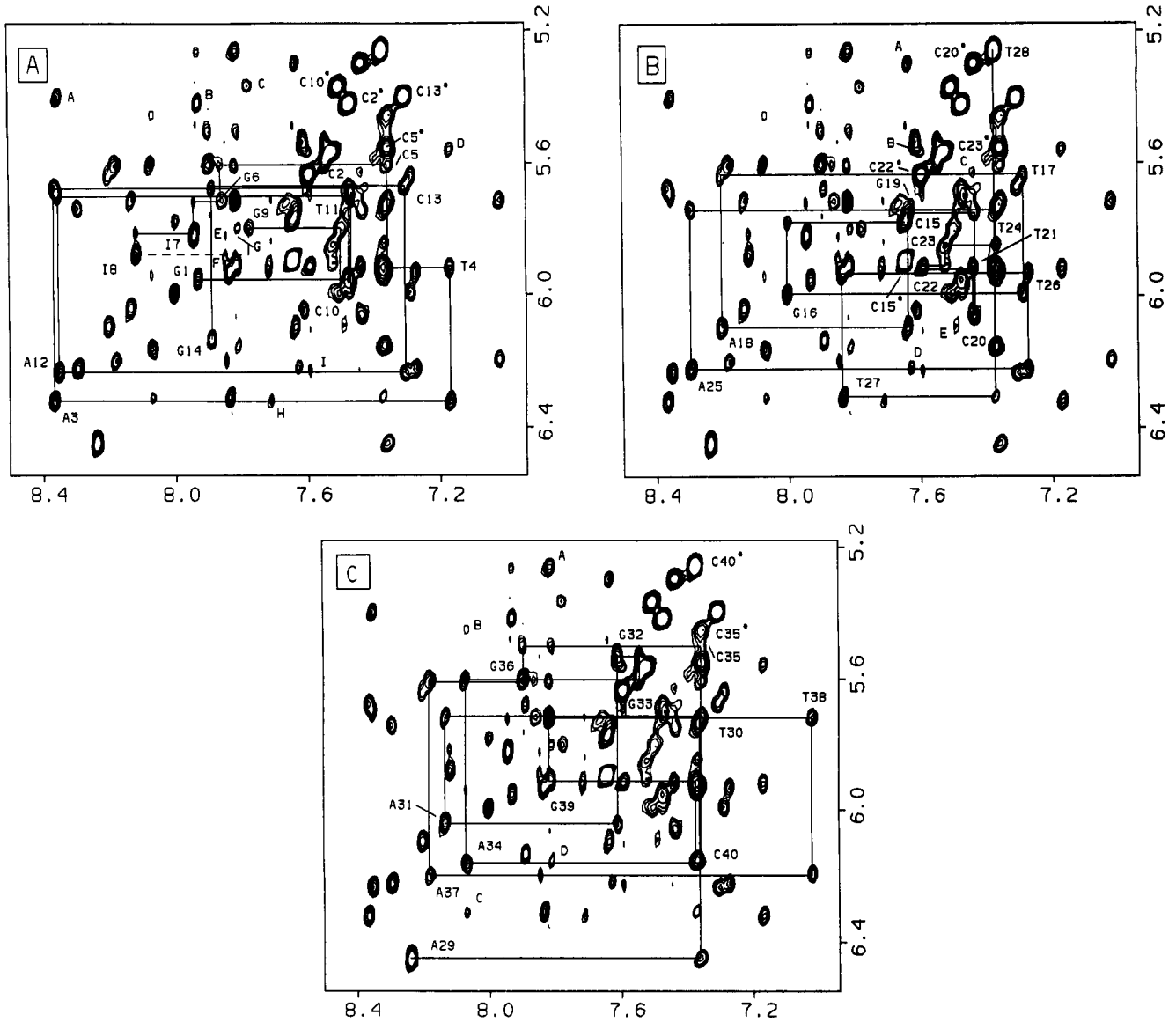

FIGURE 7: Expanded contour plot of the NOESY experiment (200-ms mixing time) on J3II in D_2O buffer at 25 °C. The base to H1′ region of the spectrum is shown. Sequential cross peaks are traced out separately for each of the three strands. Dotted lines represent absent sequential connectivities. Assignments for the remaining labeled cross peaks are as follows. Panel A (residues 1–14): (A) A12(H8)–C13(H5), (B) G1(H8)–C2(H5), (C) G9(H8)–C10(H5), (D) T4(H6)–C5(H5), (E) [I7(H2) or I8(H2)]–I7(H1′), (F) [I7(H2) or I8(H2)]–I8(H1′), (G) [I7(H2) or I8(H2)]–G9(H1′), (H) A3(H2)–A3(H1′), (I) A12(H2)–A12(H1′). Panel B (residues 15–28): (a) G19(H8)–C20(H5), (B) C22(H6)–C23(H5), (C) T21(H6)–C22(H5), (D) A25(H2)–A25(H1′), (E) A18(H2)–A18(H1′). Panel C (residues 29–40): (A) G39-(H8)–C40(H5), (B) A34(H8)–C35(H5), (C) A29(H2)–T27(H1′), (D) A34(H2)–A34(H1′).

(H6)–C7(CH_3) cross peak is labeled C7*. A new NOE cross peak of interest (peak B) is also indicated in the figure. This represents an NOE between the methyl group of C7 and the H2 proton of A37, located within the minor groove of stem I. This C7 methyl group also shows NOEs to C5(H1′) and T38(H1′), both of which are in the minor groove of stem I, as well as to an unidentified H4′ proton, possibly belonging to G6. This new information confirms our earlier supposition that C7 does not stack within the helical portions of the junction. Instead, we now discover that the base is looped out from the helix, positioned along or within the minor groove of the preceding stem.

We also discovered that the substitution of a 5-methylcytosine base at position 7 of J3CC led to some serendipitous changes in the chemical shifts of protons on neighboring residues. As a result, several newly resolved NOE cross peaks were visible. One of these is shown as peak A in Figure 6A. It represents an NOE between G6(H8) and T21(CH_3). In the original junction, J3CC, the G6(H8) proton overlaps with G16(H8), obscuring the G6(H8)–T21(CH_3) cross peak underneath the much stronger G16(H8)–T17(CH_3) connectivity. This new finding, coupled with the prior observation that the bases of A34 and C35 are most likely stacked upon each other, suggests that stems I and III of the junction may be colinear, combining to form a quasi-continuous helix within the molecule.

Assignment of Nonexchangeable Proton Resonances for J3II. With the assignments completed for the J3CC junction complex, the assignment of nonexchangeable proton resonances in the J3II complex was relatively straightforward. Figure 7 shows three panels of the base to H1′ region of a NOESY experiment (200-ms mixing time) on J3II in D_2O buffer at 25 °C. As was done for the J3CC junction, the sequential assignments are shown separately for the three strands in panels A–C.

In the first strand (panel A), the sequential assignments within the segment G6-I7-I8 can be traced without interruption. The absolute assignments for I7 and I8 are made

with confidence here due to the directionality of the NOE connectivity pattern in this region. There is no NOE cross peak between I8(H1′) and G9(H8). We do see other proton resonances, at 7.82 and 7.85 ppm, that show NOEs to the H1′ protons of I7, I8, and G9 (cross peaks E, F, and G, Figure 5A). These are most likely the H2 protons of I7 and I8. However, we are unable to make absolute assignments for either of these protons.

Due to the overlap of the H6 proton resonances for residues C20 and T21 (Figure 6B), it is difficult to determine the presence or absence of a sequential NOE between C20(H1′) and T21(H6). This overlap, which cannot be resolved by changing the temperature, precludes the assignment of other critical NOEs at this step. We do note that there is a moderately strong NOE between C20(H5) and T21(CH_3) in the NOESY spectrum (data not shown). In J3CC, no such NOE connectivity was seen. This represents a significant difference in the NOE cross peak patterns of the two junctions.

For the A34-C35 base step in the third strand, there is a weak NOE between A34(H8) and C35(H5) (cross peak B in Figure 6C). The A34(H1′)–C35(H6) NOE is obscured in this experiment by the overlapping NOE cross peak between C40(H1′) and C40(H6). However, C40 is a terminal base whose proton chemical shifts are quite tempreature sensitive. We therefore repeated the NOESY experiment on J3II at 35 °C, and have obtained a spectrum in which we observe a weak but well-resolved A34(H1′)–C35(H6) NOE. Nevertheless, judging by both the small number and the weaker strength of the NOE cross peaks between residues A34 and C35, the interaction between these two bases is much weaker in the J3II junction than it is in J3CC.

The other finding of note for this segment is the chemical shift of the H6 and H5 protons of C35. These resonances are located at 7.36 and 5.46 ppm, respectively. This represents a substantial downfield shift when compared with the corresponding resonances of the J3CC junction. This change, as well as the weaker nature of the A34-C35 NOE connectivities, suggests that the geometry of this base step is quite sensitive to the identity of the unpaired nucleotides across the branch point.

In Figure 8, we have plotted portions of the base to H2′/2″ and methyl region from the same NOESY experiment on J3II. The NOE connectivities between the H2′/2″ and H8 protons for the G6-I7-I8-G9 segment are indicated in panel B. Intraresidue NOE cross peaks are identified by residue, while sequential NOEs are marked by asterisks. Once again we find no sequential NOE cross peak between I8 and G9. One additional NOE of interest is shown in panel A of Figure 8. The arrow indicates an NOE connectivity between G6-(H8) and T21(CH_3). This NOE, also observed in the methylated J3CC junction, is highly suggestive of a helical stacking interaction between stems I and III. Thus, despite significant differences between the NOESY spectra of J3CC and J3II, it appears that the stacking between stems I and III is conserved.

The chemical shifts of all nonexchangeable protons assigned for the J3II junction in D_2O buffer at 25 °C are listed in Table II.

Assignment of Nonexchangeable Proton Resonances of J3AA. We also ran and analyzed NOESY experiments on the junction J3AA with two unpaired adenines instead of inosines at the branch point. Figure 9 shows expanded contour plots from the 200-ms-mixing-time NOESY spectrum of this molecule at 25 °C in D_2O buffer. We have traced out the sequential connectivities for residues 1–14 within the base to

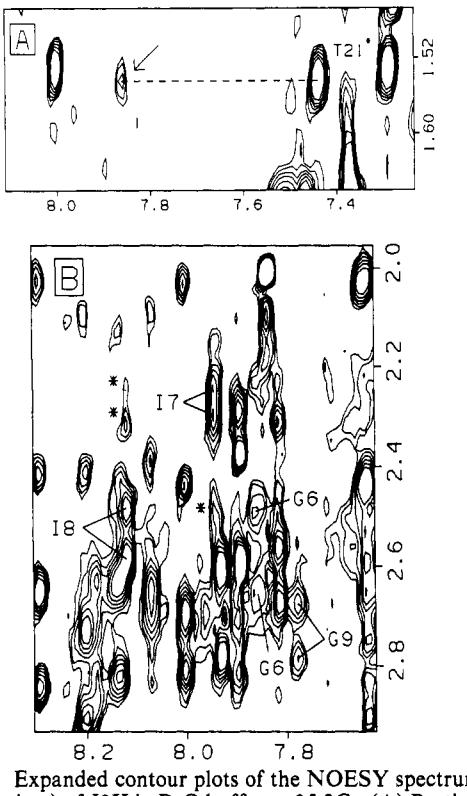

FIGURE 8: Expanded contour plots of the NOESY spectrum (200-ms mixing time) of J3II in D_2O buffer at 25 °C. (A) Portion of the base to methyl region of the spectrum. The T21(H6)–T21(CH_3) cross peak is labeled. The arrow represents an NOE between G6-(H8) and T21(CH_3). (B) Portion of the base to H2′/2″ region of the spectrum detailing NOE connectivities involving the sequence G6-I7-I8-G9. Intraresidue H8–H2′/2″ cross peaks are labeled, while interresidue cross peaks are indicated by asterisks. No NOE connectivities are seen for the I8-G9 base step.

H1′ region (panel B). The results are strikingly similar to those from J3II, the only significant difference being the chemical shift of A7(H1′) in J3AA versus that of I7(H1′) in J3II. As was the case for J3II, we can trace out the NOE connectivities for the sequence G6-A7-A8 within J3AA. However, cross-peak overlap makes it difficult to determine whether there are any visible NOE connectivities between A8 and G9. These NOEs, if present, are clearly quite weak. Furthermore, the H2 protons of A7 and A8 both resonate at 7.74 ppm, overlapping with A34(H2). NOE interactions from these protons to others within the bulge site are therefore difficult to discern. We also note that, in this case, the A34-(H1′)–C35(H6) NOE is well-resolved at 25 °C (data not shown), with a similar cross-peak intensity to that seen in J3II.

In Figure 9A the base to methyl region of the NOESY spectrum is shown. The most significant finding here is the presence of a cross peak between C20(H6) and T21(CH_3) (peak B, Figure 9A). In the NOESY spectrum of J3II, no such cross peak was visible due to the overlap between C20-(H6) and T21(H6). However, we also see an NOE between G6(H8) and T21(CH_3) (peak A, Figure 9A), similar to that seen in J3II. This finding makes it difficult to decide whether J3II and J3AA possess a similar conformation with respect to coaxial stacking of the helical stems. The potentially dynamic nature of base pairing at the branch point of J3AA might explain the unusual NMR finding. This idea is examined in more detail in the Discussion section.

The chemical shifts of all nonexchangeable protons assigned for J3AA in D_2O buffer at 25 °C are listed in Table III.

Table II: Nonexchangeable Proton Chemical Shift Assignments for the J3II Junction in D_2O Buffer at 25 °C

	chemical shifts (ppm)						
base	H6/H8	H5/CH_3	H2	H1′	H2″	H2′	H3′
G1	7.94			5.95	2.79	2.61	4.85
C2	7.48	5.42		5.68	2.50	2.17	4.91
A3	8.37		7.72	6.33	3.00	2.74	5.06
T4	7.17	1.43		5.92	2.44	2.03	4.86
C5	7.36	5.56		5.61	2.24	1.87	4.81
G6	7.86			5.72	2.65	2.50	4.80
I7	7.95		7.82[a]	5.82	2.31	2.25	4.69
I8	8.12		7.84[a]	5.88	2.59	2.49	4.88
G9	7.78			5.80	2.80	2.68	4.87
C10	7.51	5.37		5.99	2.53	2.13	4.74
T11	7.47	1.68		5.71	2.49	2.19	4.92
A12	8.36		7.60	6.24	2.89	2.75	5.07
C13	7.31	5.40		5.68	2.30	1.87	4.80
G14	7.89			6.14	2.38	2.60	4.67
C15	7.65	5.90		5.78	2.44	2.03	4.72
G16	8.01			6.00	2.81	2.70	5.00
T17	7.29	1.54		5.65	2.42	2.12	4.89
A18	8.21		7.49	6.10	2.91	2.74	5.08
G19	7.64			5.76	2.60	2.43	4.97
C20	7.44	5.30		6.06	2.47	2.31	4.80
T21	7.44	1.55		5.92	2.48	2.14	4.81
C22	7.60	5.64		5.91	2.48	2.23	4.82
C23	7.55	5.57		5.85	2.48	2.12	4.75
T24	7.37	1.68		5.74	2.42	2.03	4.88
A25	8.30		7.63	6.23	2.85	2.66	4.98
T26	7.28	1.46		5.94	2.19	2.08	4.81
T27	7.84	2.02		6.31	2.11	1.79	4.72
T28	7.38	1.37		5.26	2.00	1.65	4.46
A29	8.24		8.07	6.46	3.27	3.02	4.91
T30	7.36	1.40		5.72	2.44	2.14	4.86
A31	8.14		7.45	6.05	2.83	2.64	5.00
G32	7.62			5.54	2.64	2.51	4.96
G33	7.55			5.61	2.64	2.40	4.98
A34	8.07		7.81	6.17	2.70	2.65	4.96
C35	7.36	5.46		5.51	2.29	1.91	4.82
G36	7.90			5.61	2.82	2.72	5.01
A37	8.19		7.85	6.20	2.89	2.63	5.00
T38	7.03	1.37		5.72	2.32	1.89	4.80
G39	7.82			5.91	2.68	2.57	4.96
C40	7.37	5.27		6.16	2.21	2.21	4.49

[a] H2 protons of I7 and I8 were not distinguished.

DISCUSSION

Formation of Three-Way Junctions. We have designed a system in which two DNA oligomers, a hairpin loop with dangling ends and a complementary strand, may combine to form a three-way junction with six base pairs in each arm and two unpaired bases at the branch point. We have made three junctions with either purines or pyrimidines as the unpaired bases. Gel electrophoresis experiments demonstrate that these strands do combine in a one-to-one stoichiometry to form DNA junctions under appropriate ionic conditions. The junctions with either unpaired purines or unpaired pyrimidines behave similarly in native polyacrylamide gels. However, these experiments are sensitive only to changes in the end-to-end distance between helical arms. In molecules with very short arms such as are found in the three-way junctions, conformational differences are unlikely to cause any significant change in electrophoretic mobility.

Assignment of Nonexchangeable Protons in the Three-Way Junctions. Sequential resonance assignments for a molecule as large as our junctions pose a special problem due to the extensive cross-peak density in the NOESY spectrum. To aid in the assignment process, we designed the nucleotide sequence of stems I and II to coincide with a series of bulge-loop duplexes previously studied in this laboratory (Rosen et al., 1992a,b). In these studies, structural distortions of the

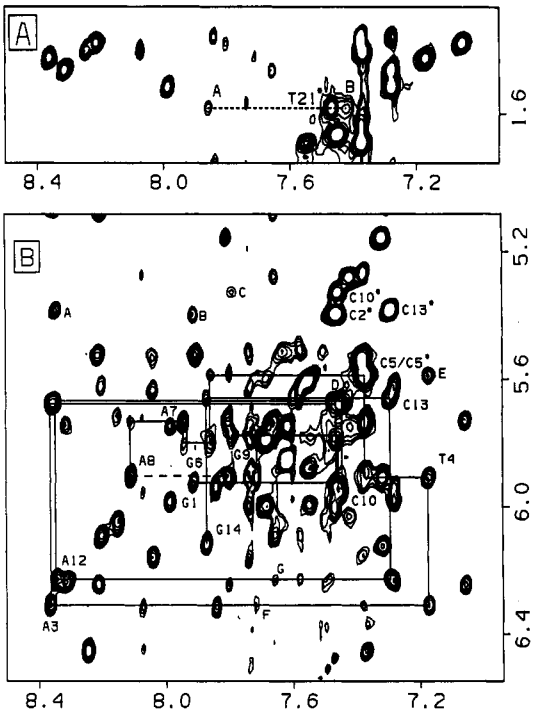

FIGURE 9: Expanded contour plots of the NOESY spectrum (200-ms mixing time) of J3AA in D_2O buffer at 25 °C. (A) Base to methyl region. The H6-CH_3 NOE for residue T21 is labeled with an asterisk. Cross peak A represents the G8(H8)–T21(CH_3) NOE. Peak B represents the C20(H6)–T21(CH_3) NOE. (B) Base to H1′ region. Sequential connectivities for residues 1–14 are indicated. Cytidine H6–H5 NOEs are labeled with asterisks. Additional cross peaks are labeled as follows: (A) A12(H8)–C13(H5), (B) G1(H8)–C2(H5), (C) G9(H8)–C10(H5), (D) C2(H6)–C2(H1′) and T11-(H6)–T11(H1′), (E) T4(H6)–C5(H5), (F) A3(H2)–A3(H1′), (G) A12(H2)–A12(H1′).

DNA helix were localized to within one or two base pairs of the bulge loop. By assuming that the conformational rearrangements in a three-way junction are similarly localized to the branch point site, we could easily trace the NOE connectivity pattern for these two stems. We also designed the hairpin loop in stem III to coincide with a sequence previously studied by Blommers et al. (1989, 1991). Using their prior work, as well as the unusual NOE pattern from the TTTA tetraloop, we were able to complete the assignments for stem III as well.

Despite these favorable circumstances, the assignment process was at times hampered by severe overlap in the NOESY spectrum. In many cases it was necessary to compare one side of the diagonal to its image in order to take advantage of the superior resolution in the $\omega 2$ dimension for each proton type. NOEs between base (H8 or H6) and sugar (H1′, H2′/2″, and H3′) protons were assigned in conjunction with the NOE cross-peak patterns within the sugar moieties themselves. For mapping the intraresidue connectivities within the sugars, we found that data from a short-mixing-time NOESY (50 ms) was superior to data from COSY-type experiments, possibly due to the large line widths of the proton resonances. Stereospecific assignments for the H2′/2″ proton pair were made on the basis of the relative intensity of the H1′–H2′ and H1′–H2″ NOE cross peaks in the 50-ms-mixing-time NOESY spectrum, assuming the latter should always be greater at this short mixing time. For residues in which such a determination was not possible, comparisons were made to previously reported assignments of the component duplex stem regions (Blommers et al., 1991; Rosen et al., 1992a).

Conformational Features of J3CC. The nonexchangeable proton NMR resonance assignments for J3CC demonstrate

Table III: Nonexchangeable Proton Chemical Shift Assignments for the J3AA Junction in D_2O Buffer at 25 °C

	chemical shifts (ppm)						
base	H6/H8	H5/CH_3	H2	H1′	H2″	H2′	H3′
G1	7.91			5.93	2.79	2.60	4.85
C2	7.47	5.40		5.68	2.48	2.18	4.91
A3	8.37		7.72	6.31	2.99	2.73	5.06
T4	7.17	1.44		5.91	2.41	1.99	4.85
C5	7.38	5.60		5.59	2.20	1.83	4.80
G6	7.86			5.80	2.60	2.41	4.80
A7	7.95		7.74	5.74	2.28	2.11	4.77
A8	8.11		7.74	5.91	2.65	2.56	4.91
G9	7.79			5.78	2.73	2.64	4.90
C10	7.46	5.33		5.96	2.51	2.10	4.75
T11	7.46	1.68		5.68	2.48	2.15	4.91
A12	8.35		7.58	6.23	2.88	2.74	5.07
C13	7.30	5.39		5.67	2.29	1.95	4.79
G14	7.87			6.12	2.60	2.38	4.67
C15	7.62	5.86		5.75	2.43	2.02	4.71
G16	7.99			5.99	2.80	2.69	4.99
T17	7.28	1.53		5.63	2.41	2.10	4.89
A18	8.20		7.49	6.09	2.92	2.75	5.08
G19	7.66			5.74	2.61	2.48	4.97
C20	7.42	5.29		6.03	2.45	2.32	4.80
T21	7.47	1.59		6.01	2.50	2.20	4.85
C22	7.69	5.79		6.00	2.50	2.29	4.85
C23	7.55	5.61		5.89	2.50	2.13	4.79
T24	7.37	1.70		5.75	2.41	2.03	4.89
A25	8.31		7.66	6.24	2.86	2.67	4.99
T26	7.28	1.47		5.94	2.19	2.10	4.82
T27	7.84	2.02		6.32	2.11	1.80	4.73
T28	7.38	1.37		5.27	2.01	1.66	4.46
A29	8.25		8.08	6.46	3.27	3.03	4.91
T30	7.37	1.42		5.72	2.44	2.15	4.87
A31	8.16		7.51	6.05	2.83	2.65	5.01
G32	7.63			5.51	2.63	2.50	4.97
G33	7.58			5.64	2.60	2.41	4.94
A34	8.04		7.74	6.16	2.65	2.57	4.94
C35	7.38	5.54		5.52	2.30	1.94	4.81
G36	7.91			5.53	2.79	2.70	5.00
A37	8.22		7.80	6.25	2.92	2.65	5.02
T38	7.06	1.39		5.73	2.33	1.92	4.83
G39	7.81			5.91	2.67	2.56	4.96
C40	7.32	5.16		6.13	2.22	2.22	4.48

that the junction consists of three right-handed, B-form helices, one of which is part of a stem–loop structure. All intra- and interresidue NOE cross peaks expected for B-form DNA are seen within these regions of the molecule. This result agrees with studies of four-way DNA junctions, in which the helices exhibit a B-DNA conformation in solution (Marky et al., 1987; Chen et al., 1991).

When the structure of multistranded DNA or RNA junctions is studied, the crucial areas of interest are at the segments that span the branch point site in the junctions. Accordingly, in our analysis of the NOESY spectrum of J3CC, we have focused our attention on the segments G6-C7-C8-G9, C20-T21, and A34-C35. Our goals have been to determine the conformational status of the unpaired bases at the branch point and to obtain information concerning the disposition of the three helices relative to each other.

The sequential NOE pattern for the two unpaired cytosines in J3CC is unusual, indicating that these residues adopt nonstandard conformation(s) within the molecule. The downfield chemical shift of the base protons from these two residues suggests that these bases may loop out from the helix into solution. This hypothesis was confirmed in the NOESY spectrum of the methylated J3CC analogue, in which NOE cross peaks were observed from the C7 methyl group to minor groove protons of stem I.

In the J3CC junction, the presence of many strong interresidue NOEs between A34 and C35 suggests that these two bases stack with one another. This makes stems I and III the most plausible candidates for colinear stacking in J3CC. If such an arrangement of the helices were taking place, one would also expect to see NOE connectivities between residues G6 and T21. Due to cross-peak density within the NOESY spectrum, we cannot see such interactions within J3CC. However, the J3CC analogue with a 5-methylcytosine base at position 7 produces a NOESY spectrum with superior cross-peak resolution. In this molecule, the G6(H8)–T21(CH_3) NOE is clearly visible. This result constitutes a strong piece of evidence in support of the colinearity of stems I and III in the junction.

The use of a methylated analogue of the J3CC junction to confirm and complete assignments raises the question of whether such a modification will perturb the structure of the molecule. Small chemical shift differences are detectable in bases at the branch point, suggesting some alteration of the conformation and/or dynamics of the molecule in this region. In one or two cases these alterations have led to serendipitous detection of new NOE cross peaks. However, we believe that there are no dramatic conformational differences between the two molecules. All chemical shift differences between these molecules (except for protons belonging to C7) are small. Furthermore, discounting those NOEs seen to the C7-Me protons, all newly discovered NOEs in the spectrum of the methylated junction have been judged by us as likely to be present but obscured in the NOESY spectrum of the original molecule.

These NMR results on the J3CC junction can be contrasted with gel electrophoresis studies on three-way junctions lacking additional bases at the branch point (Duckett & Lilley, 1990), which suggest that no helical stacking occurs and that these junctions adopt a symmetric, "Y" conformation. Other researchers (Guo et al., 1990; Lu et al., 1991) have seen evidence of an asymmetric disposition of the arms of three-stranded junctions. However, none of these studies have looked at junctions containing unpaired bases at the branch point. These bases have been shown to stabilize three-way junctions (Leontis et al., 1991). It is conceivable that the function of the unpaired bases is to relieve a conformational stress that otherwise prevents the molecule from adopting a structure in which the internal bases participate in Watson–Crick pairing while maximizing base-stacking interactions at the branch point site.

Comparison of Nonexchangeable Proton Chemical Shifts for J3CC and J3II. A residue-by-residue comparison of selected nonexchangeable proton chemical shifts for J3CC and J3II is plotted in Figure 10. The unpaired bases at the branch point and in the loop are omitted. Twelve residues are plotted in each panel so that the branch point of the junction is located in the middle of each plot. Not surprisingly, proton resonances from internal residues of the junction are most dependent on the identity of the two unpaired bases at the branch point. Interestingly, this effect is not limited to the strand containing the unpaired bases but is more diffusely spread throughout the branch point region of the molecule. This implies that conformational differences exist between the J3CC and J3II molecules that are not due solely to the disposition of the two unpaired bases at the junction.

A closer look at Figure 10 reveals several significant features. There is an upfield shift in the H8 and H1′ proton resonances of G6 and G9 when inosine bases replace the cytosines at positions 7 and 8. Proton chemical shift values in DNA are heavily dependent on nearest-neighbor interactions. The upfield shifts in residues G6 and G9 seen in J3II may reflect

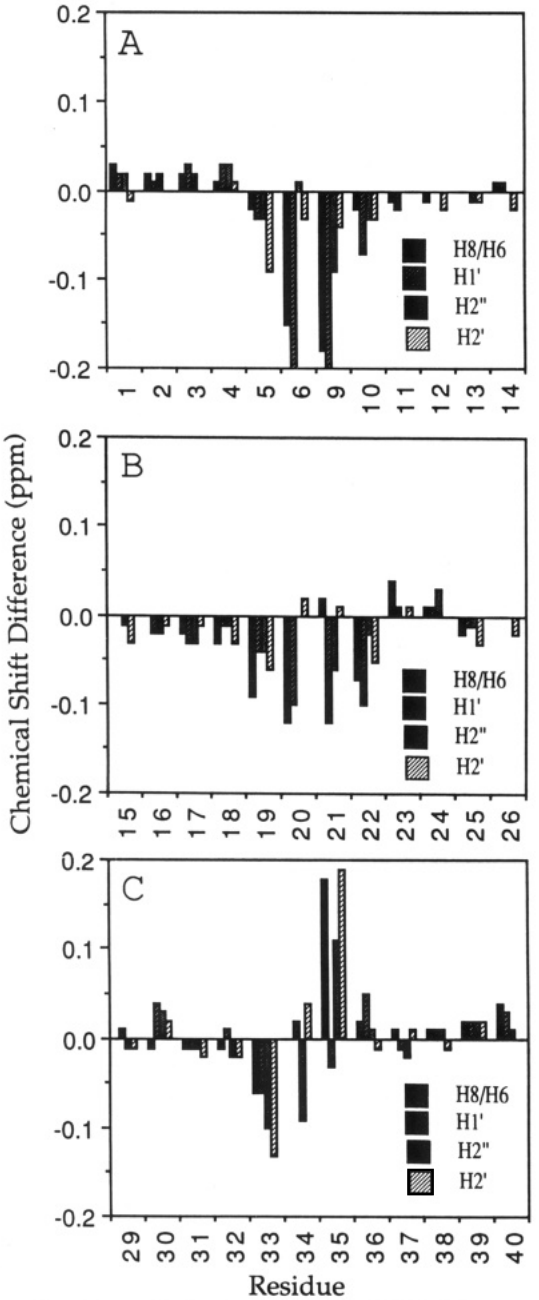

FIGURE 10: Bar graph showing the chemical shift differences at 25 °C between the base, H1′, H2′, and H2″ protons of J3II and J3CC for residues within the double-helical regions of the junctions. A positive difference indicates that the proton resonance in question is located further downfield in the J3II molecule.

the presence of stacking interactions between these guanine bases and the neighboring inosines.

A second stretch of residues at the branch point, G19–C20-T21-C22, contain proton resonances that shift upfield in J3II. Since ring current effects from pyrimidine bases within this sequence are generally weaker than those from purine bases, it is likely that one or both of the two inosine residues of J3II is interacting with some of the bases in this region as well. This indicates that, in the structure of the J3II junction, the inosine bases effect the proton chemical shifts of a number of residues on different strands.

The most striking chemical shift differences between J3CC and J3II take place at residue C35. In the J3CC molecule, the H6, H5, and H2′/2″ protons all resonate at extreme upfield positions. In 3JII, we see a downfield shift of these proton resonances to more normal values. There are two possible explanations for this observation. Ring currents from either I7 or I8 might again be responsible if the C35 residue were to lie adjacent to one of these bases in the plane of the purine ring. However, it is more likely that global conformational changes between the two junctions are the cause of this chemical shift difference. If base stacking with A34 results in the upfield C35 resonances in J3CC, as is suggested by the large number of NOE connectivities between these two bases, then any disruption of this interaction would explain the more downfield chemical shift values for proton resonances from residue C35 in the J3II junction. The smaller number of strong NOE connectivities between residues A34 and C35 of J3II supports this notion.

Comparison between J3AA and J3II. For the most part, our analysis of the NOESY spectrum of J3AA matches that of J3II. The most significant difference in the NOESY spectra of the two molecules is the resolution of C20(H6) and T21-(H6) in J3AA, with the concomitant observation of the C20-(H6)–T21(CH_3) NOE. Such an NOE might indicate the presence of a stacking interaction at this base step. However, in the case of J3AA, inspection of the sequence demonstrates that there are two alternative base-pairing schemes available to the molecule: T21 could pair with either A34 or A8. Which pairing, if either, would be energetically preferred is impossible to predict *a priori*. In J3II, the analogous pairing alternative, a T21·I8 mismatch, would be less likely to occur. For this reason, we have chosen to focus our analysis on the NOESY spectrum of J3II. In J3AA the presence of the G6(H8)–T21(CH_3) NOE assures us that the geometries of the two purine–bulge junctions are similar. The additional presence of a C20(H6)–T21(CH_3) NOE in J3AA may simply reflect the transient formation of an alternative conformation that includes a base pair between A8 and T21.

Position of Unpaired Bases in Bulge-Loop Duplexes and Three-Stranded Junctions. The tendency of bulged pyrimidines to loop out from the helix of duplex DNA (Morden et al., 1983, 1990; Kalnik et al., 1989b, 1990) seems to be echoed in the behavior of the unpaired cytidine bases in the three-way junction J3CC. In the studies of bulged pyrimidines in duplex DNA, the unpaired base could not be localized to any particular position. In contrast, we can explicitly locate the first unpaired cytosine of J3CC within or along the minor groove of stem I. This is not the first time we have observed such a phenomenon with unpaired pyrimidines in DNA. In a DNA duplex containing an abasic site, a cytosine base opposite the lesion is also located in the minor groove of one-half of the molecule (unpublished data). This phenomenon may be general to DNA. Whether unpaired pyrimidines within duplex regions of RNA will behave similarly, though, is not clear at this time.

For bulged purine residues, solution NMR studies have shown that these bases prefer to remain stacked within the helix (Patel et al., 1982; Woodson & Crothers, 1988; Kalnik et al., 1989a; Nikonowicz et al., 1990). This observation was recently extended in our laboratory to include bulge loops of two or three purine bases (Rosen et al., 1992a). The NMR results presented for J3II and J3AA support the placement of the two purine bases in the interior of the junctions. In these molecules, none of the proton resonances from the bulged bases are significantly downfield shifted, as would be expected if any of these residues were to loop out into solution. In J3II and J3AA, the H8 protons of G6 and G9 resonate further upfield than they do in J3CC. In the NOESY spectra of J3II and J3AA, we see continuous through-space connectivities within the sequences G6-I7-I8 and G6-A7-A8, respectively.

In J3AA, the presence of an NOE connectivity between A7-(H8) and A8(H8) is strongly suggestive of a stacking interaction at this base step, while in J3II, NOEs between the inosine H2 protons and nearby H1′ protons are indicative of a right-handed helical conformation in this region.

In bulge-loop duplexes, the insertion of two or more bases into the helix causes the DNA molecule to kink away from the bulge-containing strand (Rosen et al., 1992b). It has been suggested (Leontis et al., 1991) that a similar structural deformation would facilitate the formation of three-way junctions. However, in a junction such as J3II, the covalent geometry about the unpaired bases is quite different. One would therefore expect that the geometric relationship between helices in three-way junctions and bulge-loop duplexes would be different. The configuration of bases at the branch point of the purine junctions J3II and J3AA remains unclear at this time. In particular, it is difficult to imagine how G6 might stack with both T21 and I7/A7. Our NMR data does not allow us to resolve this dilemma. Therefore, our proposals regarding the branch point conformation of J3AA and J3II remain qualitative. However, it is clear that the unpaired purines in these molecules are at least partially stacked with their neighboring base pairs within the interior of the molecule. This result can be directly contrasted with that of J3CC, where one of the unpaired pyrimidines loops out from the interior of the molecule to reside within the minor groove of a preceeding stem.

Structural and Biological Effects of Unpaired Bases within Three-Way Junctions. In all three junctions studied, the NOE data suggest that stems I and III interact to form a quasi-continuous helix. However, differences in the proton chemical shifts and the NOE cross-peak pattern suggest that the identity of the unpaired residues in the junction may have an affect on the tertiary structure of the molecule. This result has important consequences for understanding the tertiary structure of larger RNA molecules, in which structural features such as multistranded junctions are commonly encountered. The 5S RNA molecule is one of the simplest cellular RNAs known. Extensive phylogenetic comparisons and chemical modification studies of natural 5S RNA and site-directed mutants have led to a consensus secondary structure in which a three-way junction is the dominant feature. A number of evolutionarily conserved, unpaired residues are located on one strand at the branch point of this junction. Elimination or substitution of these residues leads to structural alterations detectable by chemical modification and protein binding assays (Egebjerg et al., 1989; Romaniuk, 1989; Baudin et al., 1991). It has been suggested that these bases may play an importnat role in the structure and dynamics of the junction. Our results on three-way DNA junctions support this idea. Unpaired purine and pyrimidine bases appear to adopt strikingly different conformations when placed at the branch point of three-way DNA junctions. We suggest that this phenomenon may in turn affect the overall structure and dynamics of the multi-stranded DNA and RNA junctions.

CONCLUSIONS

We have demonstrated that stable three-way DNA junctions with unpaired bases at the branch point may be formed from two oligonucleotide strands. We have assigned all of the base, H1′, H2′, H2″, and H3′ protons in three junctions that differ only in the identity of the unpaired bases. The inclusion of an unusually stable four-base hairpin loop within the junction molecules has greatly aided us in the process of completing sequential proton resonance assignments. We have also demonstrated the utility of using three-dimensional homonuclear NMR experiments to help resolve ambiguous assignment possibilities in the two-dimensional NOESY spectra of complex DNA molecules.

Our results indicate that the helices of these three-way junctions retain a B-like conformation in solution. All bases at the branch point maintain an *anti* configuration about the glycosidic bond. In the junction with two unpaired cytidine residues, the bases show an unusual pattern of proton chemical shifts and NOE connectivities. The 5′ residue, C7, is clearly looped out from the interior of the molecule and resides along the minor groove of stem I. The 3′ residue, C8, may be located within the interior of the molecule but does not stack normally with its 3′ neighbor, G9.

In the junctions with either two inosine or two adenine bases at the branch point, the chemical shift and NOE patterns are more indicative of an internally stacked position for both of these residues. The NOESY spectra of these molecules demonstrate the presence of sequential NOE connectivities within these regions, leading us to propose that the unpaired bases in these molecules adopt a right-handed helical configuration and participate in some base-stacking interactions with the neighboring residues.

In both junctions, there is a strong indication of a preferred pair-wise stacking among two of the three helices. This observation should be contrasted with earlier studies in which the helices in three-way DNA junctions were shown to be symmetrically disposed in the molecule. However, these studies were done on junctions lacking bulged bases at the branch point site.

In comparing the junction molecules we have studied, we find some significant differences in proton chemical shifts and NOE cross-peak patterns. These differences indicate that the identity of the unpaired bases at the branch point may influence the tertiary structure of the molecule. This finding has implications for the role of evolutionarily conserved, single-stranded bases in determining the structure of multistranded junctions within cellular RNAs.

ACKNOWLEDGMENT

We wish to thank Dr. Clemens Anklin for technical assistance with the three-dimensional NOESY–NOESY experiment and Bruker, Inc., for the use of their AMX-600 spectrometer.

REFERENCES

Baudin, F., Romaniuk, P. J., Romby, P., Brunel, C., Westhof, E., Ehresmann, B., & Ehresmann, C. (1991) *J. Mol. Biol. 218*, 69–81.

Blommers, M. J. J., Walter, J. A. L. I., Haasnoot, C. A. G., Aelen, J. M. A., van der Marel, G. A., van Boom, J. H., & Hilbers, C. W. (1989) *Biochemistry 28*, 7491–7498.

Blommers, M. J. J., van de Ven, F. J. M., van der Marel, G. A., van Boom, J. H., & Hilbers, C. W. (1991) *Eur. J. Biochem. 201*, 33–51.

Bodenhausen, G., Vold, R. C., & Vold, R. R. (1980) *J. Magn. Reson. 37*, 93–106.

Boelens, R., Vuister, G. W., Koning, J. M. G., & Kaptein, R. (1989) *J. Am. Chem. Soc. 111*, 8525–8526.

Broker, T. R., & Doermann, A. H. (1975) *Annu. Rev. Genet. 9*, 213–244.

Chen, S.-M., Heffron, F., Leupin, W., & Chazin, W. J. (1991) *Biochemistry 30*, 766–771.

Clegg, R. M., Murchie, A. I. H., Annelies, Z., Carsten, C., Diekmann, S., & Lilley, D. M. J. (1992) *Biochemistry 31*, 4846–4856.
Cooper, J. P., & Hagerman, P. J. (1989) *Proc. Natl. Acad. Sci. U.S.A. 86*, 7336–7340.
Duckett, D. R., & Lilley, D. M. J. (1990) *EMBO J. 9*, 1659–1664.
Duckett, D. R., Murchie, A. I. H., & Lilley, D. M. J. (1990) *EMBO J. 9*, 583–590.
Egebjerg, J., Christiansen, J., Brown, R. S., Larsen, N., & Garrett, R. A. (1989) *J. Mol. Biol. 206*, 651–668.
Fasman, G. (1975) *CRC Handbook of Biochemistry and Molecular Biology*, 3rd ed., Vol. I, CRC Press, Inc., Boca Raton, FL.
Guo, Q., Lu, M., Churchill, M. E. A., Tullius, T., & Kallenbach, N. R. (1990) *Biochemistry 29*, 10927–10939.
Hare, D. R., Wemmer, D. E., Chou, S. H., Drobny, G., & Reid, B. R. (1983) *J. Mol. Biol. 171*, 319–336.
Holliday, R. (1964) *Genet. Res. 5*, 282–304.
Jensch, F., & Kemper, B. (1986) *EMBO J. 5*, 181–189.
Kalnik, M. W., Norman, D. G., Swann, P. F., & Patel, D. J. (1989a) *J. Biol. Chem. 264*, 3702–3712.
Kalnik, M. W., Norman, D. G., Zagorski, M. G., Swann, P. F., & Patel, D. J. (1989b) *Biochemistry 28*, 294–303.
Kalnik, M. W., Norman, D. G., Li, B. F., Swann, P. F., & Patel, D. J. (1990) *J. Biol. Chem. 265*, 636–647.
Leontis, N. B., Kwok, W., & Newman, J. (1991) *Nucleic Acids Res. 19*, 759–766.
Lu, M., Guo, Q., & Kallenbach, N. R. (1991) *Biochemistry 30*, 5815–5820.
Ma, R.-I., Kallenbach, N. R., Sheardy, R. D., Petrillo, M. L., & Seeman, N. C. (1986) *Nucleic Acids Res. 14*, 9745–9753.
Marion, D., & Wuthrich, K. (1983) *Biochem. Biophys. Res. Commun. 113*, 967–974.
Marky, L. A., Kallenbach, N. R., McDonough, K. A., Seeman, N. C., & Breslauer, K. J. (1987) *Biopolymers 26*, 1621–1634.
Meselson, M. S., & Radding, C. H. (1975) *Proc. Natl. Acad. Sci. U.S.A. 72*, 358–361.
Minigawa, T., Murakami, A., Ryo, Y., & Yamagishi, H. (1983) *Virology 126*, 183–193.
Morden, K. M., Chu, Y. G., Martin, F. H., & Tinoco, I., Jr. (1983) *Biochemistry 22*, 5557–5563.
Morden, K. M., Gunn, B. M., & Maskos, K. (1990) *Biochemistry 29*, 8835–8845.
Nikonowicz, E. P., Meadows, R. P., & Gorenstein, D. G. (1990) *Biochemistry 29*, 4193–4204.
Orr-Weaver, T. C., Szostak, J. W., & Rothstein, R. J. (1981) *Proc. Natl. Acad. Sci. U.S.A. 78*, 6354–6358.
Patel, D. J., Kozlowski, S. A., Marky, L. A., Rice, J. A., Broka, C., Itakura, K., & Breslauer, K. J. (1982) *Biochemistry 21*, 445–451.
Patel, D. J., Shapiro, L., & Hare, D. (1987) *Annu. Rev. Biophys. Biophys. Chem. 16*, 423–454.
Romaniuk, P. J. (1989) *Biochemistry 28*, 1388–1395.
Rosen, M. A., Live, D., & Patel, D. J. (1992a) *Biochemistry 31*, 4004–4014.
Rosen, M. A., Shapiro, L., & Patel, D. J. (1992b) *Biochemistry 31*, 4015–4026.
Seeman, N. C., Maestre, M. F., Ma, R.-I., & Kallenbach, N. R. (1984) in *The Molecular Basis of Cancer* (Rein, R., Ed.) Allan R. Liss, New York.
Sigal, N., & Alberts, B. (1972) *J. Mol. Biol. 71*, 789–793.
States, D. J., Haberkorn, B. A., & Ruben, D. J. (1982) *J. Magn. Reson. 48*, 286–292.
van de Ven, F. J. M., & Hilbers, C. W. (1988) *Eur. J. Biochem. 178*, 1–38.
Wong, Y., Mueller, J. E., Kemper, B., & Seeman, N. C. (1991) *Biochemistry 30*, 5667–5674.
Woodson, S. A., & Crothers, D. M. (1988) *Biochemistry 27*, 3130–3141.
Wuthrich, K. (1986) *NMR of Proteins and Nucleic Acids*, John Wiley & Sons, New York.